EFFECT OF LINER THICKNESS ON ACOUSTIC WAVE PROPAGATION IN DUCTS

---

by

Bassam S. Shaker

Thesis submitted to the Graduate Faculty of the

Virginia Polytechnic Institute and

State University

in candidacy for the degree of

MASTER OF SCIENCE

in

Engineering Science and Mechanics

APPROVED: _____

Chairman, Prof. A. H. Nayfeh

_____ _____

Prof. D. T. Mook Prof. J. E. Kaiser

_____

Prof. Daniel Frederick, Department Head

Blacksburg, Virginia

ACKNOWLEDGEMENT

The author wishes to express his sincere appreciation to Professors and for their counsel and guidance throughout the investigations.

The research contained in this thesis was sponsored by the Load Division of NASA Langley Research Center under and this support is gratefully acknowledged.

TABLE OF CONTENTS

LIST OF FIGURES

FIGURE PAGE

1. Introduction

The problem of reducing the internally-generated noise from a turbofan engine is becoming increasingly important due to the vast development of the aircraft industry. One approach to the solution of this problem is the use of a duct lining whose function is to absorb a significant part of the engine noise as it propagates through the ducts. The desirable mechanical properties of liners are diverse and rather stringent. The extreme temperature and pressure environment in the interior of a jet engine has required extensive experimental and theoretical research in order to develop appropriate liners. These liners are usually a combination of perforated sheets, cavities, and pieces of porous materials.

In a broad classification, liners can be divided into bulk- and point-reacting liners [1]. Bulk-reacting liners are liners that permit acoustic propagation in more than one direction. Such liners may consist of isotropic or anisotropic layers of porous materials. On the other hand, point-reacting (locally-reacting liners) permit propagation only in the direction normal to the duct walls. They usually consist of a perforated sheet or a layer of porous material followed by a honeycomb core and backed by the impervious wall of the duct. The honeycomb core consists of narrow cavities directed perpendicular to the wall which act as resonators.

Analyses of the acoustical properties of bulk-reacting liners were motivated mainly by the use of fiberglass blankets as linings in air-conditioning ducts and as parallel baffles in mufflers. Scott [2]

analyzed the effect of isotropic bulk-reacting liners on the wave propagation in a two-dimensional duct without flow; his theory was verified by several investigators [3-7]. Kurze and Vér [8] extended the analysis of Scott by considering anisotropic bulk-reacting liners. Their results show that, for low frequencies, the optimum attenuation is achieved by a bulk-reacting liner whose resistivity in the axial direction increases with frequency. This result is in agreement with the experimental observations of Bokor [4,5]. Tack and Lambert [9] formulated the problem of wave propagation in two-dimensional ducts which carry slug flow and are lined with isotropic bulk-reacting liners. Nayfeh, Sun and Telionis [10] analyzed the wave propagation in two-dimensional and circular ducts which carry sheared mean flow and are lined with isotropic bulk-reacting liners.

Analysis of the effect of point-reacting liners on the wave propagation in ducts is usually carried out either by replacing the effect of the liner by an empirical or semi-empirical impedance [numerous examples of this approach are cited in the review article 11] or by coupling the wave propagation in the duct with that in the liner [12,13]. Using the latter approach for the case of no mean flow, Morse [12] and Cremer [13] analyzed the wave propagation in a two-dimensional duct whose impervious walls are lined with a homogeneous porous material.

The purpose of this study is to analyze the wave propagation in a two-dimensional duct that carries slug flow and whose impervious walls are lined with a point-reacting liner that consists of a porous layer backed by cellular cavities. The analysis is carried out by coupling the waves in the duct with those in the porous layer and in the cavities.

2. Problem Formulation

The analytical model used in this study is a plane duct of a uniform cross section whose width is $2d^*$. The two opposite walls are acoustically treated by a point-reacting liner (see Figure 1); the liner consists of a layer of homogeneous, porous material backed by a cellular honeycomb core. The cross-sectional dimensions of the honeycomb cells are assumed to be small compared with the wavelength of the sound.

To obtain a simple demonstration of the effects of the derived liner properties, we take the mean flow within the duct to be uniform (slug flow) -- however, the analysis of the liner impedance from the wave propagation within the liner is equally applicable to the case of a sheared mean flow. In addition, the duct is assumed to be semi-infinite, so that there is no end reflection. The problem formulation requires the governing equations within the duct, the porous material, and the cellular cavities and the corresponding boundary conditions.

Governing Equations in the Duct

We introduce dimensionless quantities by using the characteristic length d^*, the undisturbed speed of sound c^*, and the density ρ_0^* as reference values. Moreover, we assume that each flow quantity is the sum of a steady mean-flow quantity and a small, unsteady acoustic quantity. Thus, if starred and unstarred quantities denote, respectively, dimensional and dimensionless quantities, we let

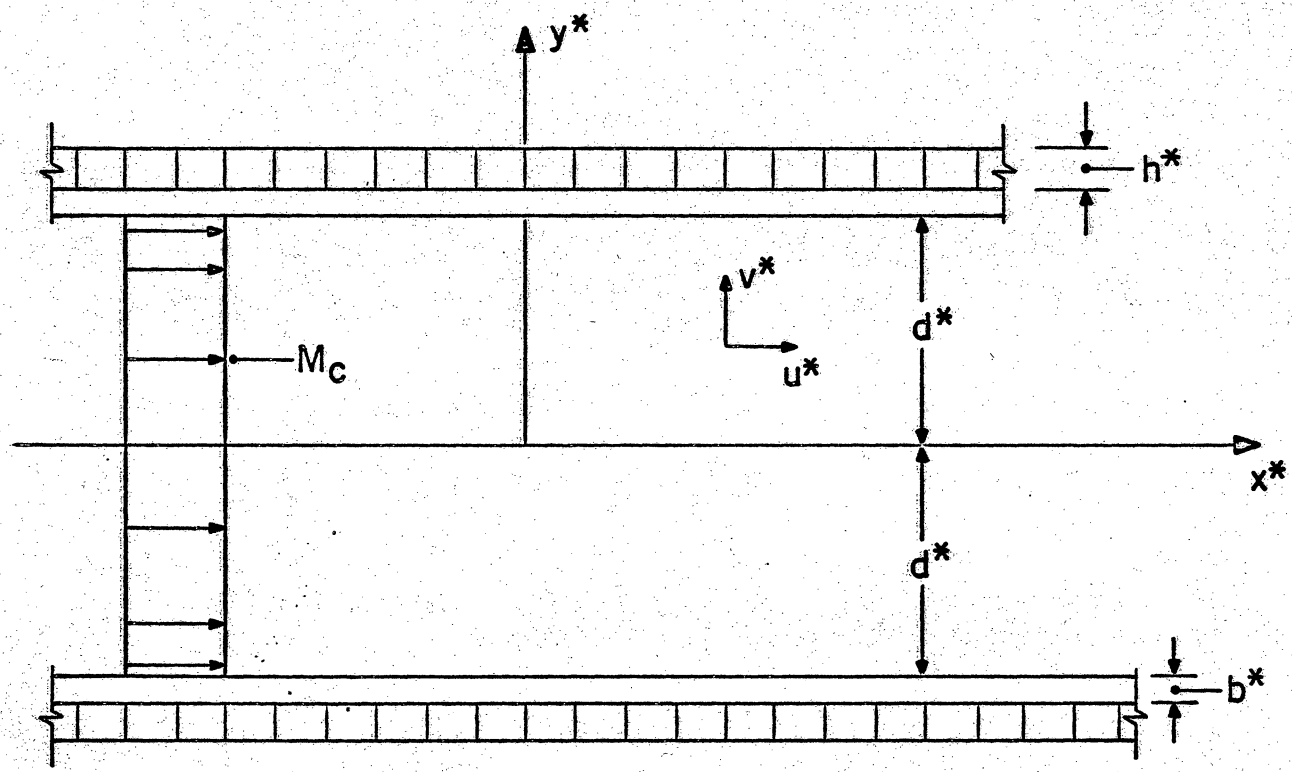

Figure 1. Duct geometry and coordinates

$$x^* = xd^*,\ y^* = yd^*,\ t^* = td^*/c^*$$

$$u^* = c^*[M + u(y)E],\ v^* = c^*v(y)E \tag{1}$$

$$\rho^* = \rho_0^*[1 + \rho(y)E],\ p^* = \rho_0^* c_0^{*2}[\gamma^{-1} + p(y)E]$$

where M is the Mach number of the uniform mean flow, γ is the gas specific heat ratio,

$$E = \exp[i(kx - \omega t)] \tag{2}$$

$\omega = \omega^* d^*/c^*$ is the dimensionless frequency, and k is the dimensionless propagation constant whose imaginary part is the attenuation coefficient.

Substituting equations (1) and (2) into the Euler equations and the isentropic equation of state and neglecting nonlinear acoustic quantities, we obtain

$$i(Mk - \omega)\rho + iku + v' = 0 \tag{3}$$

$$i(Mk - \omega)u + ikp = 0 \tag{4}$$

$$i(Mk - \omega)v + p' = 0 \tag{5}$$

$$p = \rho \tag{6}$$

where primes denote differentiation with respect to y. Then, eliminating u, v, and ρ from equations (3)-(6), we have

$$p'' + [(Mk - \omega)^2 - k^2]p = 0 \tag{7}$$

Governing Equations in the Cavities

The governing equations for the sound propagation in the cellular cavities can be obtained from those governing the flow in the duct.

Since there is no mean flow within the cavities, we set M = 0 in equations (3)-(7). In addition, we assume that the acoustic disturbance in the cavities consists of plane waves only, propagating normal to the wall -- this assumption is a consequence of the small cross-sectional dimensions of the cellular cavities. Thus with no wave propagation in the x-direction, we set k = 0 in equations (3)-(7). The acoustic disturbance within the cavities is then described by

$$u = 0 \tag{8}$$

$$-i\omega v + p' = 0 \tag{9}$$

and

$$p'' + \omega^2 p = 0 \tag{10}$$

Governing Equations in the Porous Material

We assume the porous material to be rigid, homogeneous, and partitioned to prevent axial flow. Employing the above assumptions and the dimensionless quantities which were defined in equations (1) and (2), we find that the acoustic field in the porous material is governed by [14]

$$(\sigma - i\omega\rho_e)v + p' = 0 \tag{11}$$

$$-i\omega\Omega\rho + v' = 0 \tag{12}$$

$$p = c_e^2\rho \tag{13}$$

where Ω is the porosity, $\rho_e = s/\Omega$ is the dimensionless effective density, s is the structure factor [15], $\sigma = \sigma^* d^*/\rho_0^* c^*$ is the dimensionless resistivity, and c_e is the dimensionless effective speed of sound. In

general, c_e is a complex number; it is real only at high frequencies (above 1000 Hz) and at low frequencies (below 100 Hz). Note that ρ_e, Ω, and σ are not independent but are related; however, their interdependence is complicated so that, in general, they are determined separately [11]. Equations (11)-(13) can be combined into

$$p'' + \kappa_p^2 p = 0 \tag{14}$$

where

$$\kappa_p^2 = \omega(s\omega + i\sigma\Omega)/c_e^2 \tag{15}$$

Boundary Conditions

Since the problem is symmetric, it is sufficient to consider the upper half of the duct and to use either of the following boundary conditions at the duct centerline:

$$p = 0 \quad \text{for antisymmetric modes} \tag{16a}$$

$$p' = 0 \quad \text{for symmetric modes} \tag{16b}$$

As a result of the velocity vanishing in the cavity at the impervious walls

$$v = 0 \quad \text{at} \quad y = 1 + b + h \tag{17}$$

Although the viscosity is neglected in the duct and in the cavities, it cannot be neglected near the boundaries where the viscous effects are important. With very small viscosity, the mean boundary layers can be approximated by vortex sheets across which the pressure and the particle displacement are continuous. We denote by $y = 1 + \eta_1 E$ and $y = 1 + b + \eta_2 E$ the positions of the vortex sheets that separate the flow in the duct from that in the porous material and the flow in the porous material from that in the cavities. The linearized forms of the

continuity of pressure and particle displacement across these vortex sheets are

$$p = p_p \quad \text{at } y = 1 \tag{18}$$

$$v + i(\omega - Mk)\eta_1 = 0 \quad \text{at } y = 1 \tag{19}$$

$$v_p + i\omega\eta_1 = 0 \quad \text{at } y = 1 \tag{20}$$

$$p_p = p_c \quad \text{at } y = 1 + b \tag{21}$$

$$v_p = v_c \quad \text{at } y = 1 + b \tag{22}$$

where the quantities with subscripts c and p refer, respectively, to the cavities and porous material, and those quantities without subscript refer to the duct.

3. Eigenvalue Equation and Liner Admittance

The solution of equation (7) that satisfies the boundary condition (16b) is

$$p = a_1 \cos \kappa y \quad \text{for symmetric modes} \tag{23}$$

where a_1 is an arbitrary constant and

$$\kappa^2 = (Mk - \omega)^2 - k^2 \tag{24}$$

Hence, from equation (5), we see that

$$v = - ia_1\kappa(Mk - \omega)^{-1}\sin \kappa y \tag{25}$$

The solutions of equations (9) and (10) that satisfy the boundary condition (17) are

$$p_c = a_2 \cos[\omega(y - 1 - b - h)] \tag{26}$$

$$v_c = ia_2 \sin[\omega(y - 1 - b - h)] \tag{27}$$

where a_2 is another arbitrary constant. Finally, the general solution of equations (11) and (14) is

$$p_p = a_3 \cos[\kappa_p(y + \phi)] \tag{28}$$

$$v_p = a_3\kappa_p(\sigma - i\omega\rho_e)^{-1}\sin[\kappa_p(y + \phi)] \tag{29}$$

where a_3 and ϕ are arbitrary constants.

Imposing the boundary conditions (21) and (22) at the cavity-porous material interface, we obtain

$$\tan[\kappa_p(1 + b + \phi)] = -(\omega\rho_e + i\sigma)\kappa_p^{-1} \tan(\omega h) \tag{30}$$

The specific acoustic admittance of the liner, $\beta = v_p/p_p$ at $y = 1$, is obtained from equations (28) and (29) as

$$\beta = \kappa_p(\sigma - i\omega\rho_e)^{-1} \tan [\kappa_p(1 + \phi)]$$

or, using equation (30) to eliminate the constant ϕ,

$$\beta = -\,i\left[\tan \omega h + \frac{\Omega\omega}{\kappa_p c_e^2} \tan \kappa_p b\right]\left[1 - \frac{\kappa_p c_e^2}{\Omega\omega} \tan \omega h \tan \kappa_p b\right]^{-1} \tag{31}$$

To apply this liner admittance to the slug flow in the duct, the boundary conditions (18)-(20) at the duct-porous material interface are imposed to obtain

$$\kappa \tan \kappa = -\,i(Mk - \omega)^2\, \omega^{-1} \beta \tag{32}$$

for the symmetric modes. The analysis of the antisymmetric modes yields

$$\kappa \cot \kappa = i(Mk - \omega)^2\, \omega^{-1} \beta \tag{33}$$

Equations (32) and (33), together with (24), are the characteristic equations for the eigenvalue k of symmetric and antisymmetric modes propagating in a plane duct that carries a slug flow.

Equations (31) and (15) give the specific admittance of the liner as a function of the sound frequency ω, the cavity depth h, and properties of the porous material, Ω, c_e, b, s, and σ. However, the specific admittance of the liner actually depends on only three dimensionless groups of the porous-material properties:

$$R = \sigma b \tag{34a}$$

$$\omega_o = \sigma/\rho_e = \sigma\Omega/s \tag{34b}$$

and

$$\omega_1 = c_e^2/\Omega b \tag{34c}$$

In terms of these properties, equation (31) can be written as

$$\beta = \frac{(\kappa_p b \cot \kappa_p b) + (\omega/\omega_1) \cot \omega h}{R(1 - i\omega/\omega_o) + (\kappa_p b \cot \kappa_p b) i \cot \omega h} \tag{35a}$$

where

$$\kappa_p b = \left[iR(1 - i\omega/\omega_o)\omega/\omega_1\right]^{1/2} \tag{35b}$$

In previous studies of wave propagation in ducts lined with a porous facing sheet that is backed by cellular cavities, the specific admittance of the liner has been modelled by the semi-empirical formula

$$\beta = \frac{1}{R(1 - i\omega/\omega_0) + i \cot \omega h} \tag{36}$$

This formula assumes that the impedances of the facing sheet and of the cavities are additive, that the resistance of the facing sheet, R, is a constant, and that the reactance of the facing sheet is a linear function of the frequency ω. This approximate formula can be obtained from the general formulas (35) as a restrictive special case. In the limit $b \to 0$, with R, ω_0 and ω fixed, equations (35) reduce to equation (36). Hence, equation (36), which is widely used in the literature, can be interpreted as an approximation for thin porous facing sheets. Note, however, that keeping ω_0 and R fixed while letting $b \to 0$ implies that $\sigma = O(b^{-1})$ and $s/\Omega = O(b^{-1})$, which are unrealistic. Moreover, for small but finite values of b, neglecting the term $\omega/\omega_1 = \omega\Omega b/c_e^2$ is valid only for small values of ω, and the resulting formula (36) can be expected to be inaccurate at moderate and large values of ω. The numerical results of the next section include comparisons of the attenuation rates that are obtained from the two formulas.

4. Numerical Results

The solution to equations (32), (33) and (24) has been obtained by using a Newtonian iteration scheme to find the eigenvalue κ corresponding to a variety of liner properties. The modes are identified at low frequencies and thereafter the eigenvalue of a given mode is required to vary continuously with the frequency. The numerical results are of three types: (1) the results for no backing cavity are used to verify the analysis by comparison with previously published results for locally-reacting porous liners [8]; (2) the effects of the depth of the cavity backing and the thickness of the porous material are demonstrated for constant material properties; (3) the attenuation rates predicted from the approximate formula (36) are compared with those predicted from the general formula (35a) in order to determine the importance of the detailed modelling of the wave propagation in the porous material.

Case of no backing cavity

In the absence of a backing cavity, the specific admittance predicted by equation (35a) becomes

$$\beta = - \frac{i\omega}{\omega_1 \kappa_p b \cot \kappa_p b}$$

It should be noted that the approximate formula, equation (36), is applicable neither to this case nor to the case of half-wave-length resonance of the cavities, $\omega h \to \pi$, since it predicts a rigid wall in both instances.

Kurze and Ver [8] have examined both point- and bulk-reacting porous

materials, and have calculated the attenuations produced in a plane duct with a thick liner of Fiberglas Superfine B100 for the case of no mean flow. For comparison with their results, we take $s = 1.4$, $\sigma = 1.0$, $\Omega = 0.95$, $c_e = 1.0$, and $b = 1.0$ in the expressions for the specific admittance. Figure 2 gives the attenuation rate of the lowest symmetric mode for no mean flow and, in addition, for cases of upstream and downstream propagation. The no-mean-flow results agree quantitatively with Kurze and Vér's results for a point-reacting liner up to $\omega = 7$; above $\omega = 7$, the second mode (not shown) becomes the least attenuated, and the data for the second mode agree with the results of Kurze and Vér. Thus, equations (35) reduce to the correct form in the limit as $h \to 0$.

Figure 2 also shows that the attenuation rate depends quite strongly on the mean flow. The peak attenuation frequencies shift to lower values for upstream propagation and to higher values for downstream propagation. In addition, upstream propagation increases the attenuation rate in the first peak, but decreases it in the second peak; downstream propagation has an opposite effect. Figure 3 shows similar results for the lowest anti-symmetric mode. Again, the results are very sensitive to changes in the mean-flow Mach number.

The band-width of the first peak in the attenuation can be varied by changing the flow resistivity, as shown by Figure 4 in which the resistivity has been increased to $\sigma = 10$. The convective effects of the mean flow -- a shift in the tuning frequency and a decrease in attenuation with increasing Mach number -- are clearly shown. These effects have been discussed previously [16,17] for liners described by equation (36).

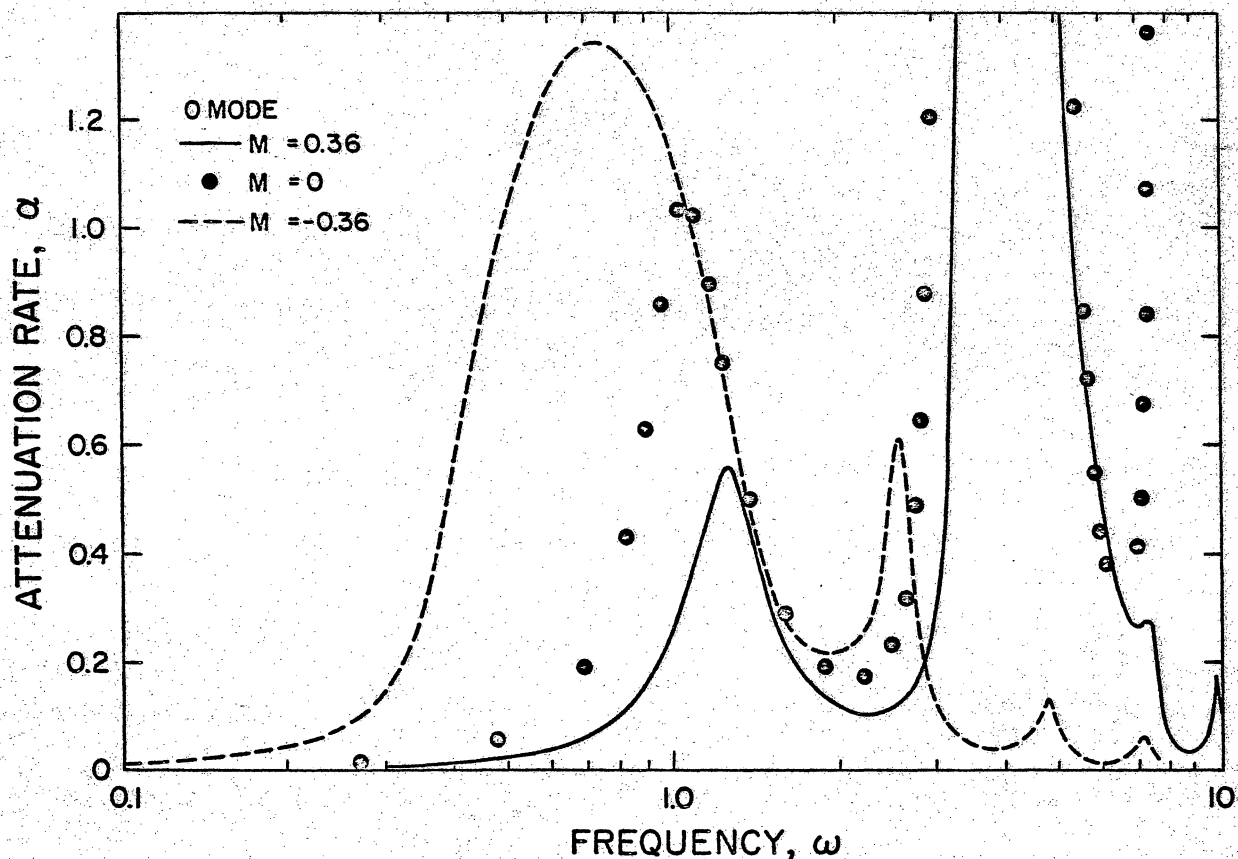

Figure 2. Attenuation rates of the lowest symmetric mode for a thick liner with no backing cavity; $\sigma = 1.0$, $b = 1.0$, $\Omega = 0.95$, $s = 1.4$, $c_e = 1.0$, $h = 0$.

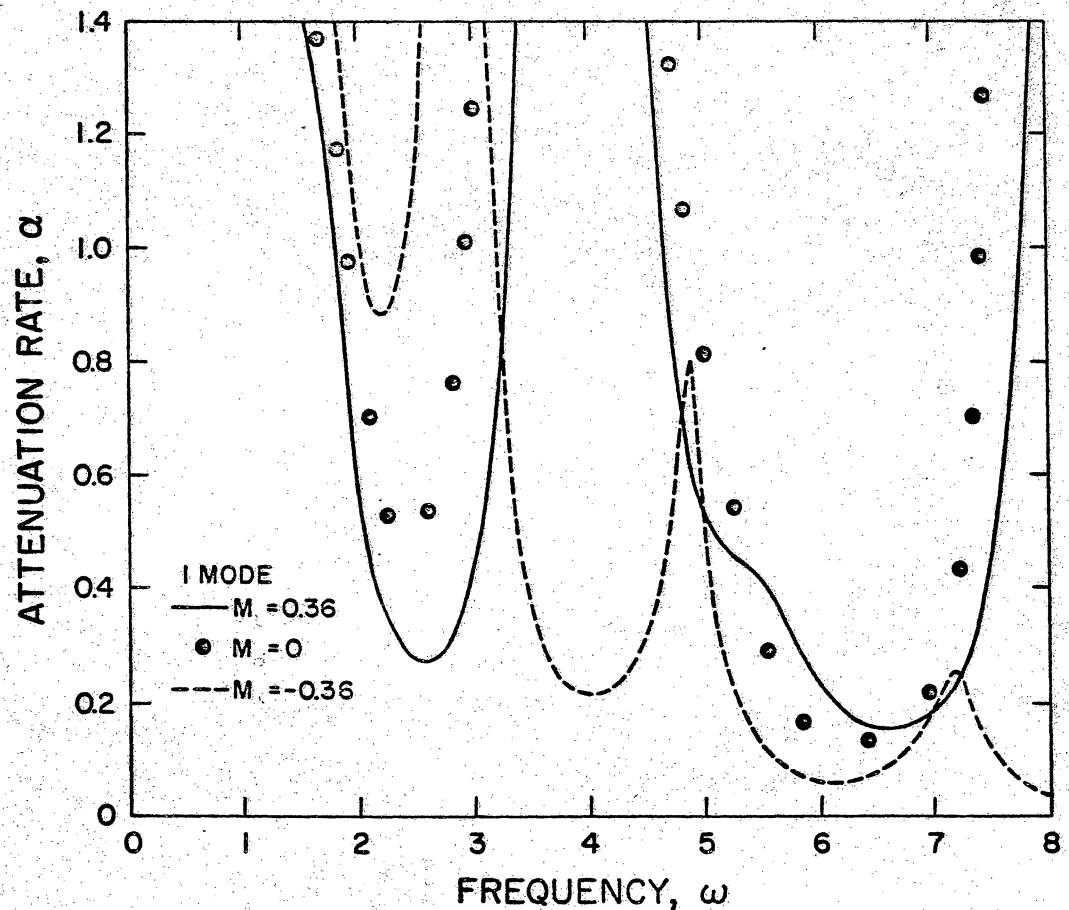

Figure 3. Attenuation rates of the lowest anti-symmetric mode for a thick liner with no backing cavity; $\sigma = 1.0$, $b = 1.0$, $\Omega = 0.95$, $s = 1.4$. $c_e = 1.0$, $h = 0$.

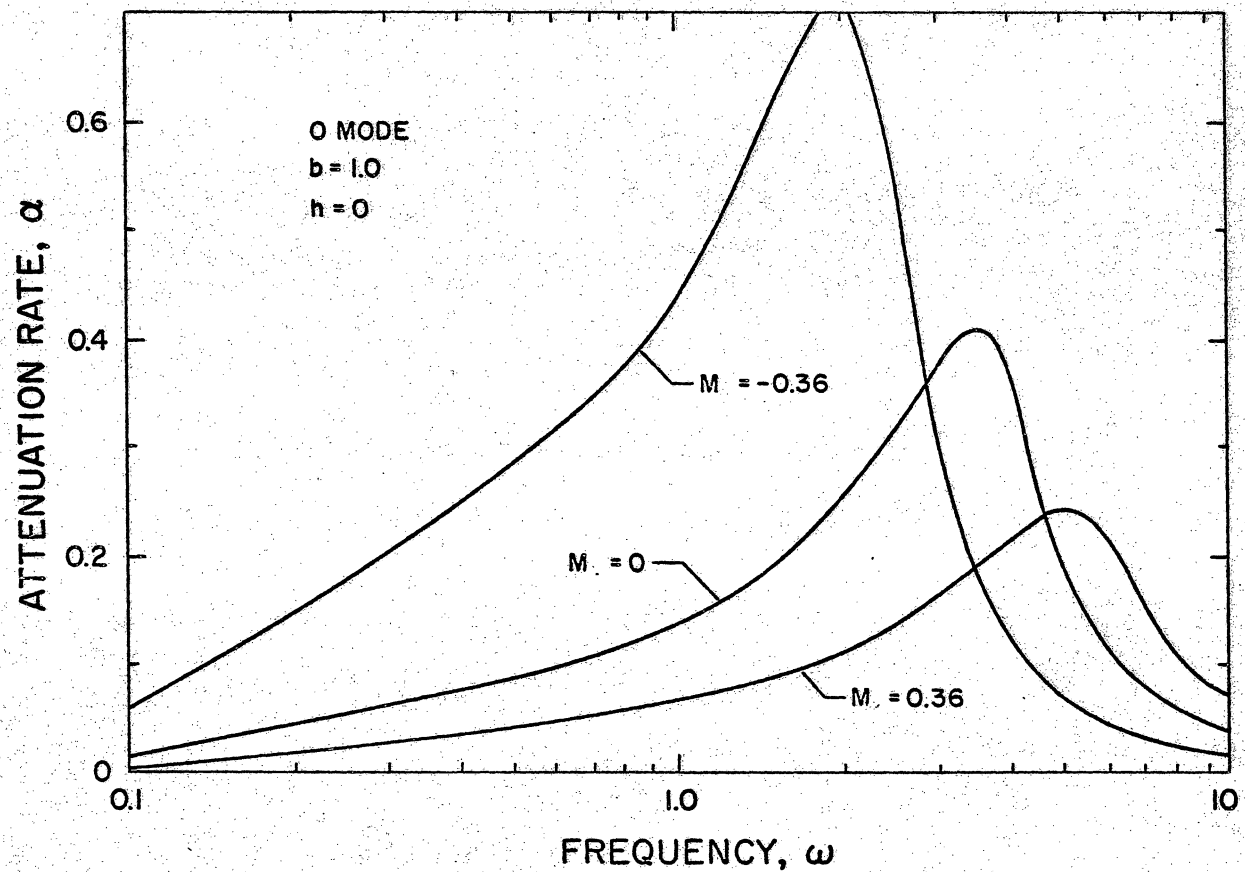

Figure 4. Effect of the mean flow on the attenuation of the lowest symmetric mode for a thick liner with no backing cavity; $\sigma = 10$, $b = 1.0$, $\Omega = 0.95$, $s = 1.4$, $c_e = 1.0$, $h = 0$.

For such liners , the tuning frequency is taken to be a function of the cavity depth and mean-flow Mach number. However, the results of Figures 2 and 4 illustrate that the material properties can have considerable influence if the porous layer is not thin.

Influence of liner dimensions

In this section, we examine the influence of variations in the cavity depth and thickness of the porous layer for fixed material properties. The material properties are taken to be $\sigma = 10$, $s = 1.4$, $\Omega = 0.95$ and $c_e = 10/11$ (a value slightly less than the free-field, isentropic value), the mean-flow Mach number is 0.36, and the liners vary from thin to thick (.03 to .50 of the duct half width).

The influence of cavity depth on the attenuation rates of the two lowest symmetric and antisymmetric modes are shown in Figures 5 and 6, respectively, for a thin porous sheet, $b = .02$. Although the net resistance of the facing sheet is small ($R = \sigma b = 0.2$), the attenuation of the first two modes can be increased to substantial values by increasing the cavity depth and thus bringing the liner closer to quarter wave-length resonance. However, except at very low frequencies, the second and third modes are more critical for these flow conditions, and their response to increases in the cavity depth is less favorable. Initially, the attenuation increases with increasing cavity depth; however, at higher frequencies it reaches a maximum and then decreases with further increases in cavity depth.

The results for the zero mode that are shown as broken lines in Figures 5 and 6 correspond to frequencies for which there is no down-

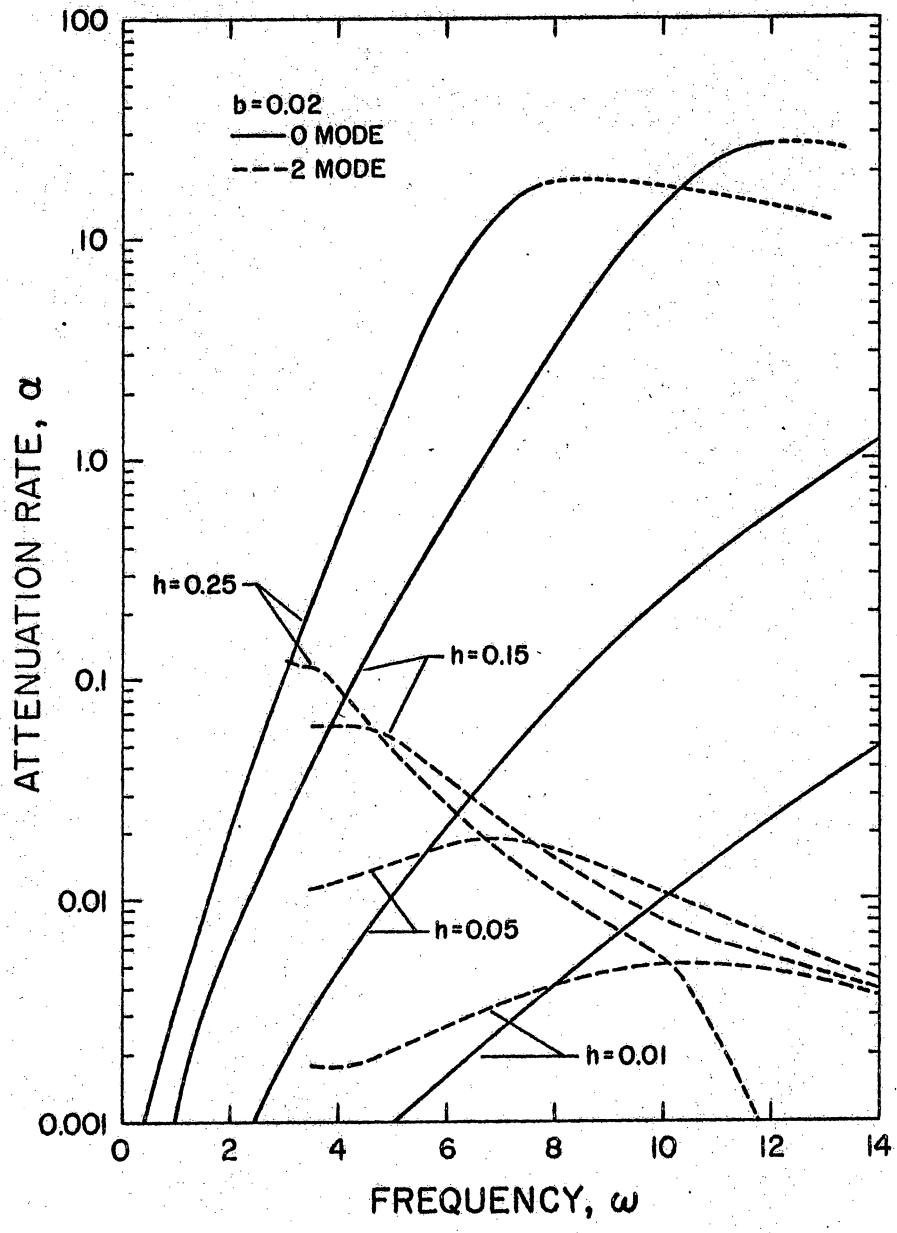

Figure 5. Effect of the cavity depth on the attenuation spectra of the two lowest symmetric modes for a thin porous sheet; σ= 10, b = .02, Ω = 0.95, s = 1.4, c_e = 0.91, M = 0.36.

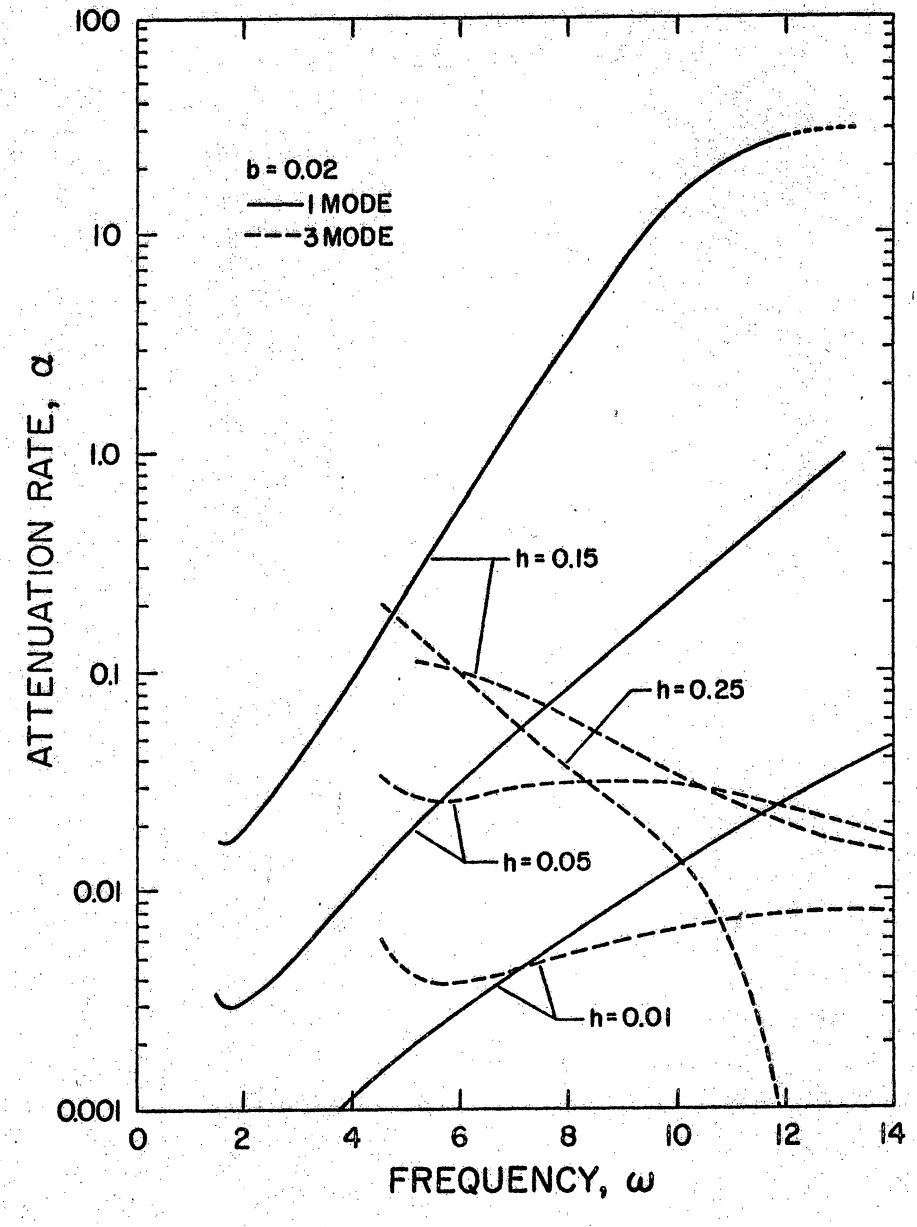

Figure 6. Effect of the cavity depth on the attenuation spectra of the two lowest antisymmetric modes for a thin porous sheet; $\sigma = 10$, $b = .02$, $\Omega = 0.95$, $s = 1.4$, $c_e = 0.91$, $M = 0.36$.

stream-propagating solution. That is, as the frequency increases the zero mode approaches a standing wave and then begins to propagate upstream. Thus this mode exhibits a cutoff phenomenon; at higher frequencies, the mode may begin propagating downstream again (an example is shown in Figure 10).

The overall low attenuation levels for the second and third modes can be improved by using a porous material of greater resistivity. This is illustrated for the symmetric case by Figure 7, which gives the attenuation as a function of resistivity. It can be seen that the attenuation of the second mode is less frequency dependent than is that of the zero mode over the entire range of resistivity. The abrupt crossover of the two modes at $\omega = 10$ and $\sigma \approx 110$ occurs as a consequence of the specific admittance being close to a value that produces a multiple root of equation (32); the occurance of such roots has been discussed at some length by Testor [18] and by Zorumski and Mason [19].

Figures 8 and 9 show the influence of the thickness of the porous facing sheet for a case of a very shallow cavity, $h = 0.01$. The specific admittance of the liner depends upon the three material parameters R, ω_0, ω_1, and two of the three, R and ω_1, are affected by a change in the facing-sheet thickness, b. An increase in the value of b increases the attenuation of the two lowest modes but is somewhat less effective than an increase in the cavity depth: the attenuation tends to reach a maximum and then decreases with further increases in the value of b. However, for the second and third modes, the increase in the thickness of the porous material produces a significant improvement in the attenuation levels and is far more effective than is an increase in the cavity depth.

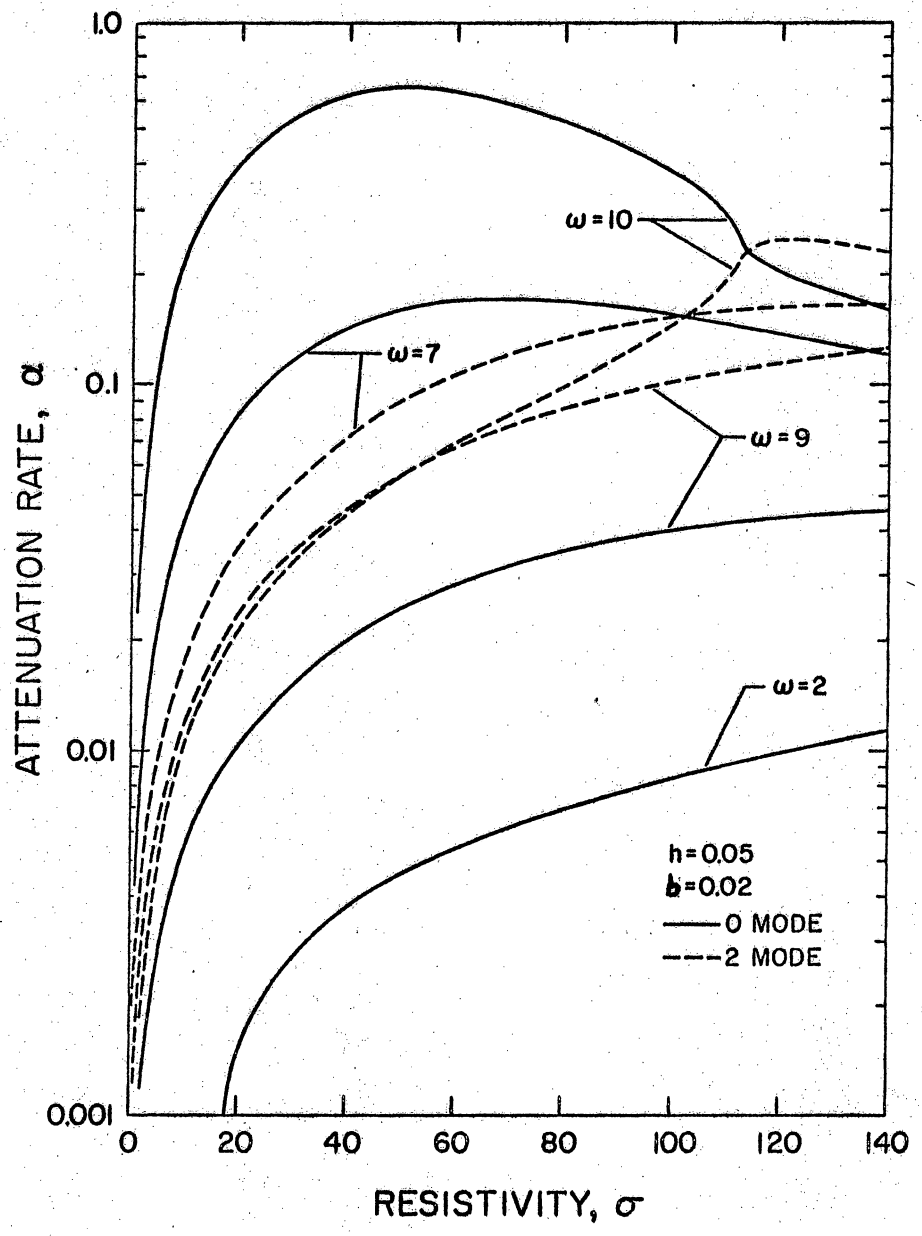

Figure 7. Influence of resistivity on the attenuation rates of the two lowest symmetric modes; b = 0.02, h = 0.05, Ω = 0.95, s = 1.4, c_e = 0.91, M = 0.36.

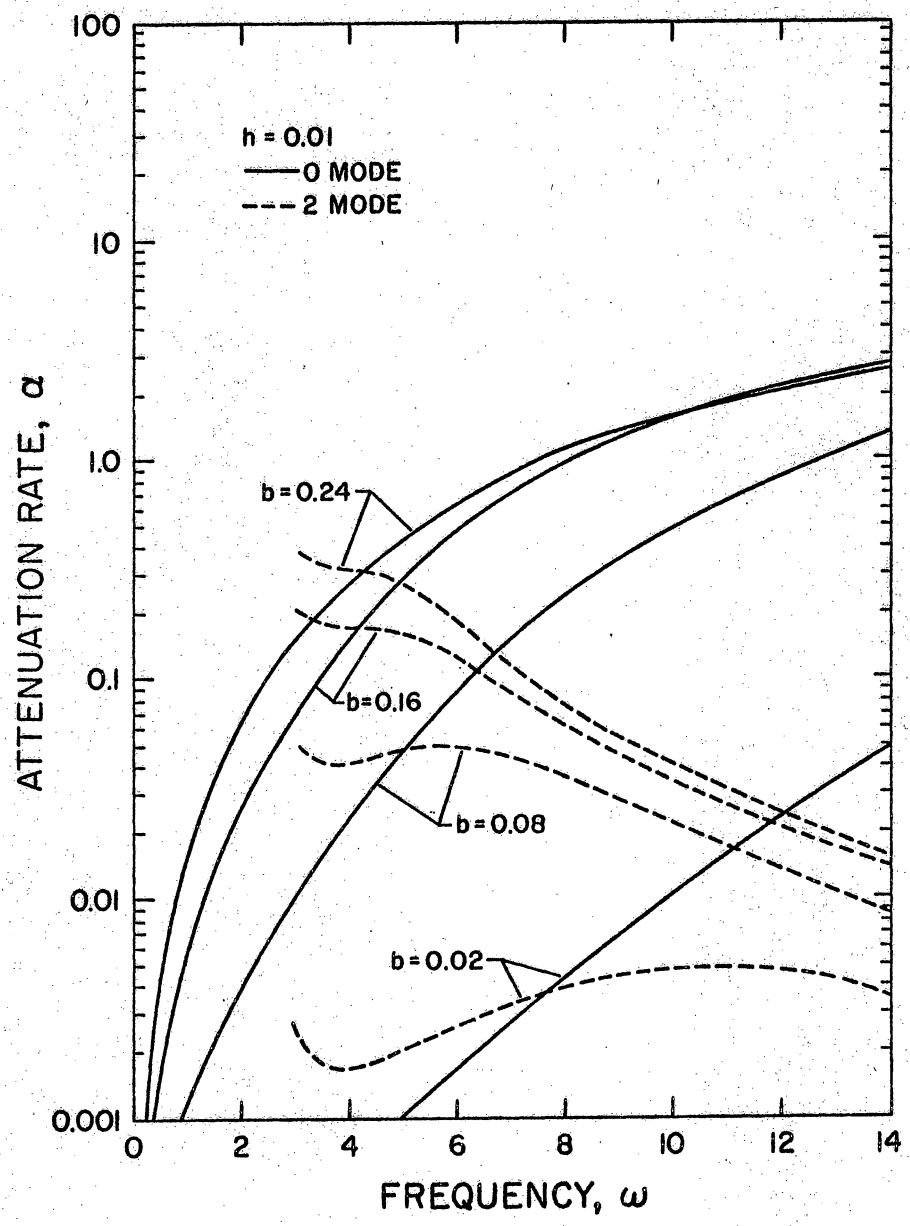

Figure 8. Effect of the porous-sheet thickness on the attenuation spectra of the first two symmetric modes for a shallow cavity; h = 0.01, σ = 10, Ω = 0.95, s = 1.4, c_e = 0.91, M = 0.36.

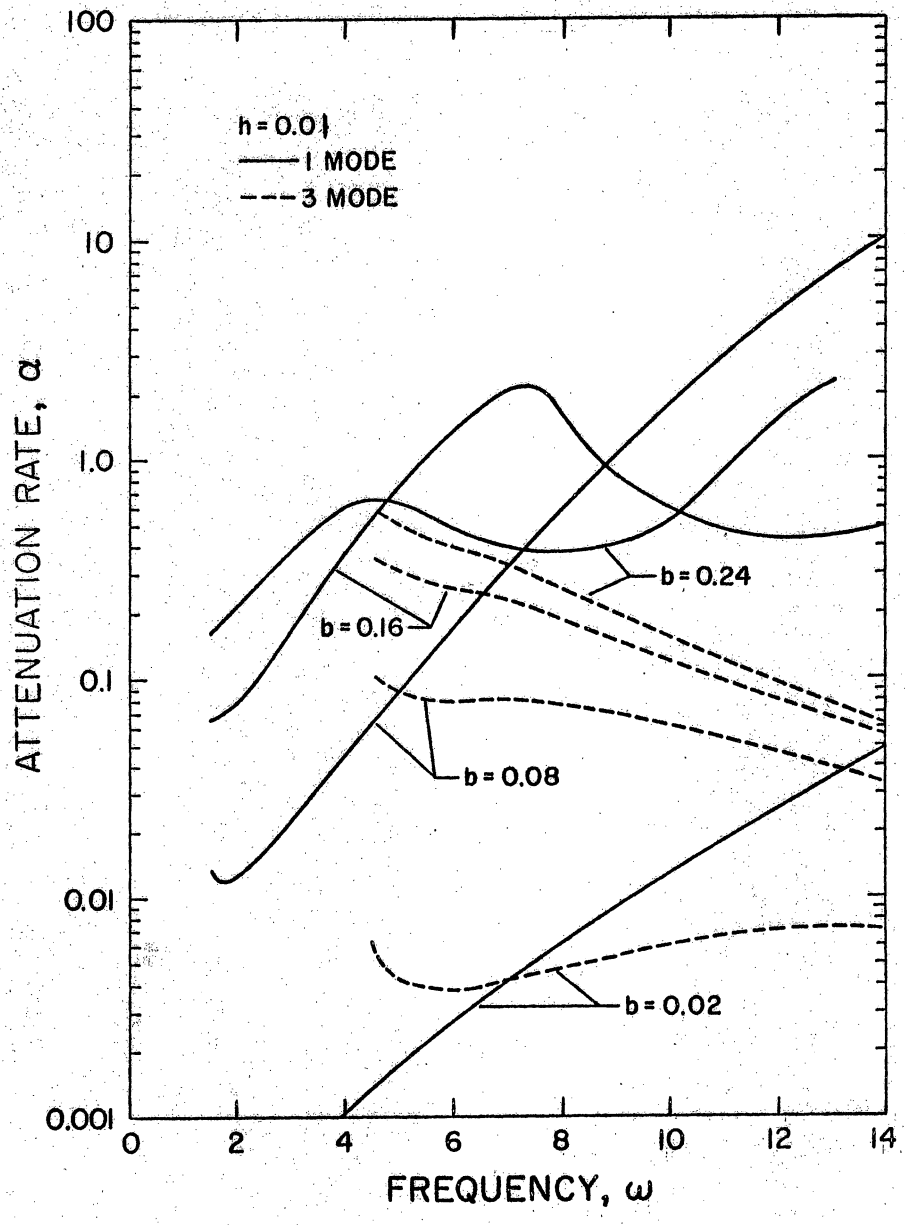

Figure 9. Effect of the porous-sheet thickness on the attenuation spectra of the first two antisymmetric modes for a shallow cavity; $h = 0.01, \sigma = 10, \Omega = 0.95, s = 1.4, c_e = 0.91, M = 0.36$.

Finally, the influence of the facing-sheet thickness is shown for a case of moderately deep cavities, h = 0.1, in Figures 10 and 11. It can be seen that increases in the thickness of the porous material above a value of b = 0.16 does not produce any change in the overall attenuation level; however, the attenuation of a specific frequency can be changed significantly as a result of a shift in the peaks of the attenuation curve. Note also that the attenuation of the second mode is increased to a value greater than that of the zero mode.

Validity of the thin-facing-sheet approximation

Previous investigations of wave propagation in ducts that are lined with porous-facing-sheet cavity liners have relied on the semi-empirical formula given by equation (36) to predict the specific admittance. As noted earlier, the general formulation, equations (35), reduce to the approximate form in the limit as $b \to 0$ with R, ω, and ω_0 fixed. In this section, we wish to examine the validity of the thin-facing-sheet approximation for use with liners of finite dimensions.

The attenuation rates predicted with the use of the two formulas are compared in Figures 12 - 14 as the porous-facing-sheet thickness progresses from thick to very thin. As is to be expected, the attenuation spectrum has a complexity that the approximate formula cannot produce when the facing sheet is sufficiently thick that an internal resonance occurs within the frequency range of interest (see Figure 12). The liner properties for this case are h = 0.1, b = 0.16, σ = 12.5, s = 1.4, c_e = 10/11 and Ω = 0.95 which correspond to R = 2, ω_0 = 8.48, and ω_1 = 5.24 for use in the general formula. The approximate formula

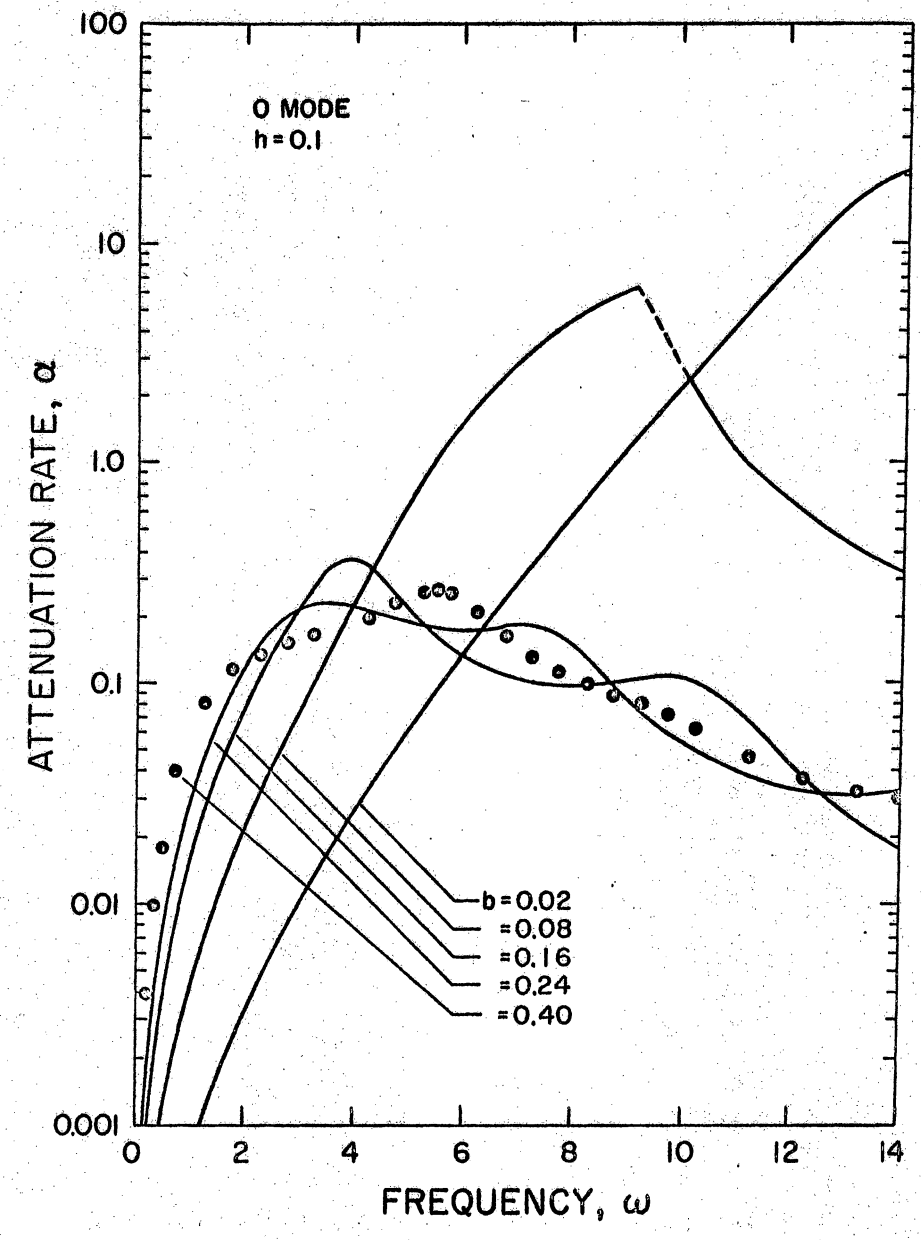

Figure 10. Effect of the porous-sheet thickness on the attenuation spectrum of the first symmetric mode for moderate cavity depth; h = 0.1, σ = 10, Ω = 0.95, s = 1.4, c_e = 0.91, M = 0.36.

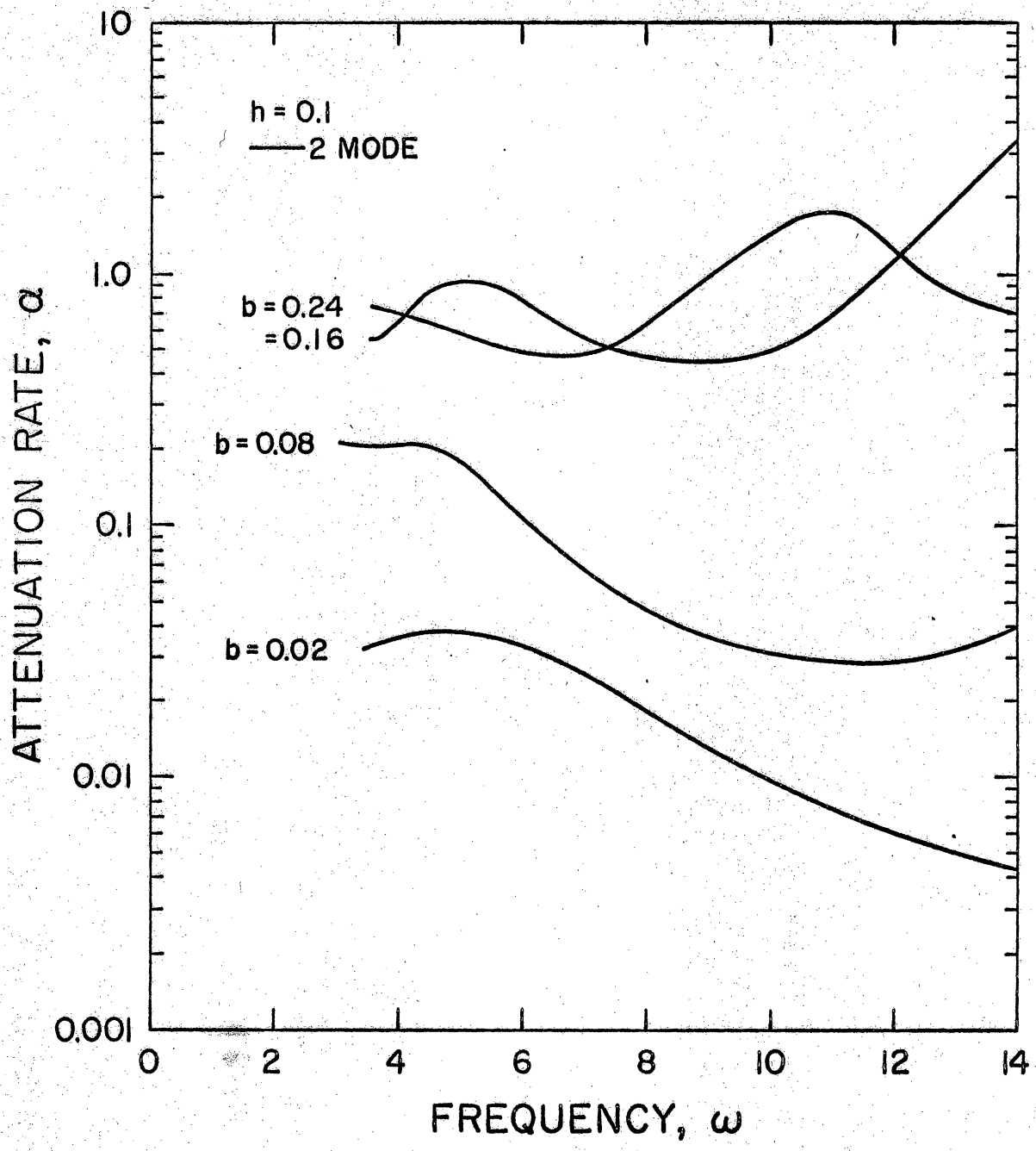

Figure 11. Effect of the porous-sheet thickness on the attenuation spectrum of the second symmetric mode for moderate cavity depth; h = 0.1, σ = 10, Ω = 0.95, s = 1.4, c_e = 0.91, M = 0.36.

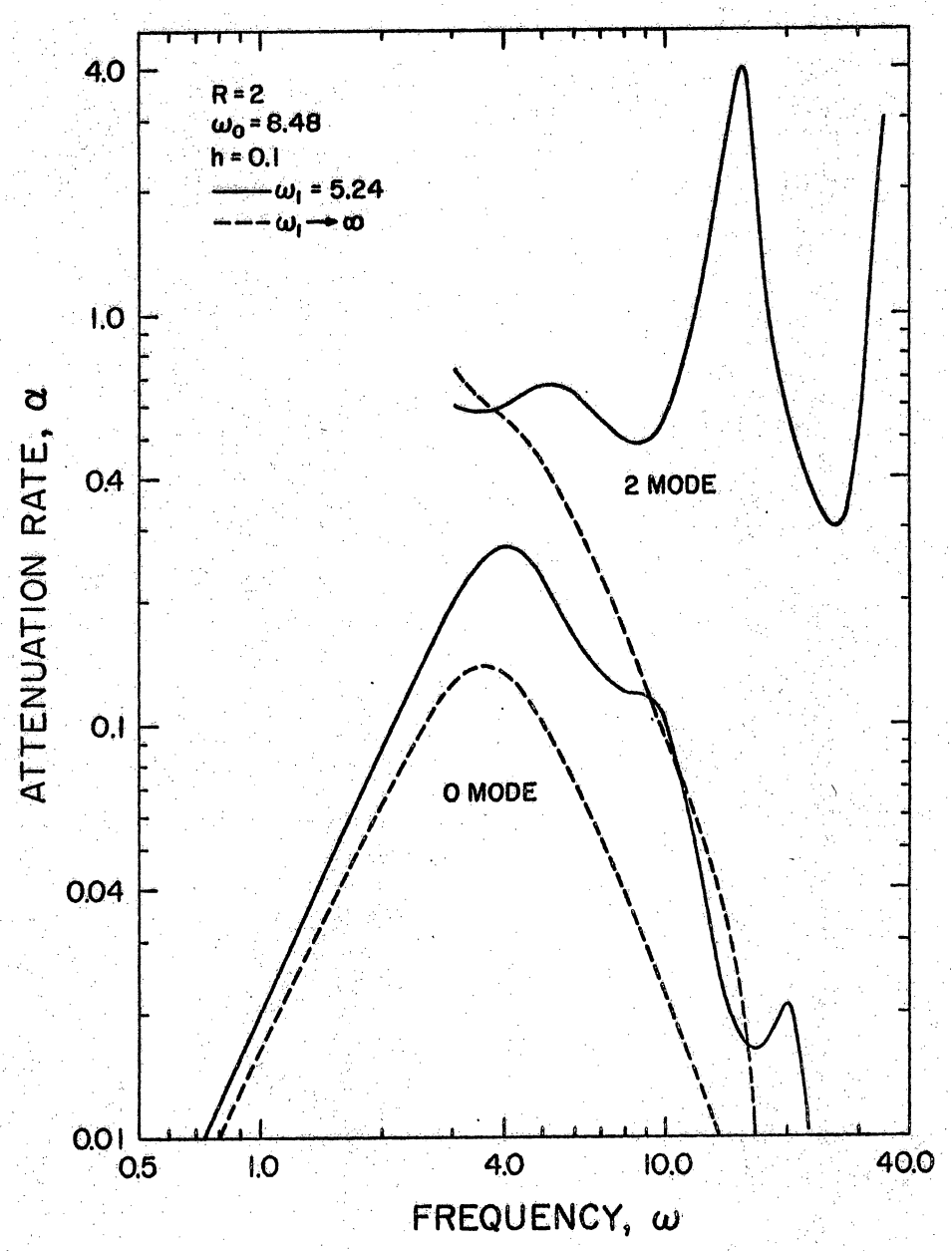

Figure 12. Comparison of the attenuation spectra predicted by the general formula (35) for the liner specific admittance to those predicted by the semi-empirical formula (36); thick facing sheet, b = 0.16, h = 0.1, σ = 12.5, Ω = 0.95, s = 1.4, c_e = 0.91, M = 0.36.

is used with the same values of R and ω_0 and corresponds to the case of $\omega_1 \to \infty$. An effective cavity depth equal to h + b/2 is used in the approximate formula. At ω = 17.45, the approximate formula predicts a "hard-wall" resonance, and the calculations were stopped at this resonance frequency. Although the general trend of the attenuation of the zero mode is predicted by the approximate formula, the overall attenuation level is substantially underpredicted and small peaks in the attenuation are overlooked. For the second mode, the approximate formula is inadequate except near the cutoff frequency.

For thinner facing sheets, a material of greater resistivity, σ, is assumed such that the resistance of the facing sheet remains at the value of R = 2; other material properties are assumed to be the same as those indicated previously, and the comparison between the exact and approximate formulas is carried out as described above. Figure 13 shows the results for a moderately thin facing sheet, b = .03 (~ 3/16 inch in a duct of 1 foot width). The attenuation curves are in general agreement over a reasonable frequency range, but the approximate formula underpredicts the peak attenuation rate by roughly thirty percent. At higher frequencies the curves diverge due to the finite thickness of the facing sheet and the approach of the "hard-wall" resonance predicted by the approximate formula (at ω = 27.3).

The results for a very thin facing sheet, b = .005, are shown in Figure 14. The agreement over the entire frequency range is very good, with approximately six percent difference at the peak attenuation of the fundamental mode; however, the thickness of the facing sheet is unrealistically small. In practice, the porous-sheet thickness and

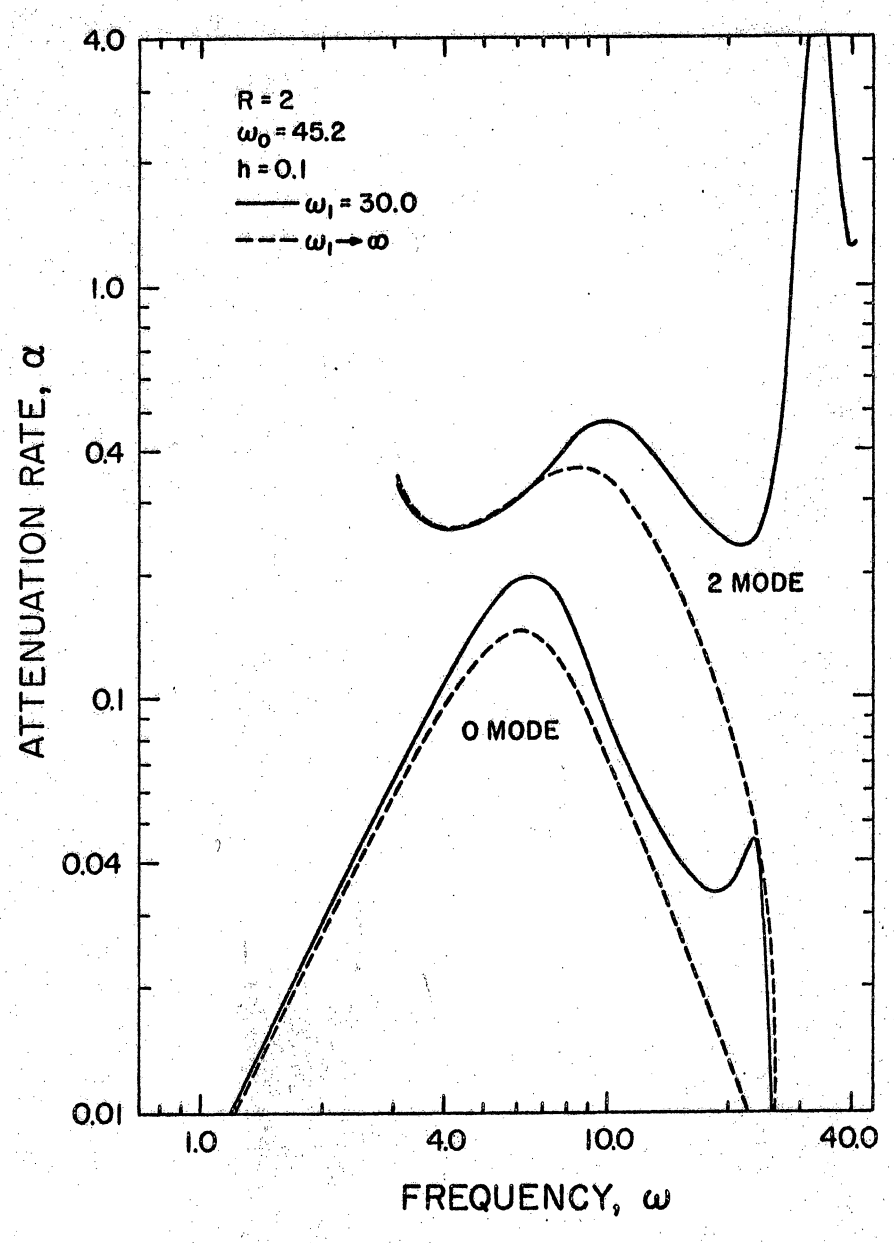

Figure 13. Comparison of the attenuation spectra predicted by the general formula (35) for the liner specific admittance to those predicted by the semi-empirical formula (36); thin facing sheet, b = 0.03, h = 0.1, σ = 200/3, Ω = 0.95, s = 1.4, c_e = 0.91, M = 0.36.

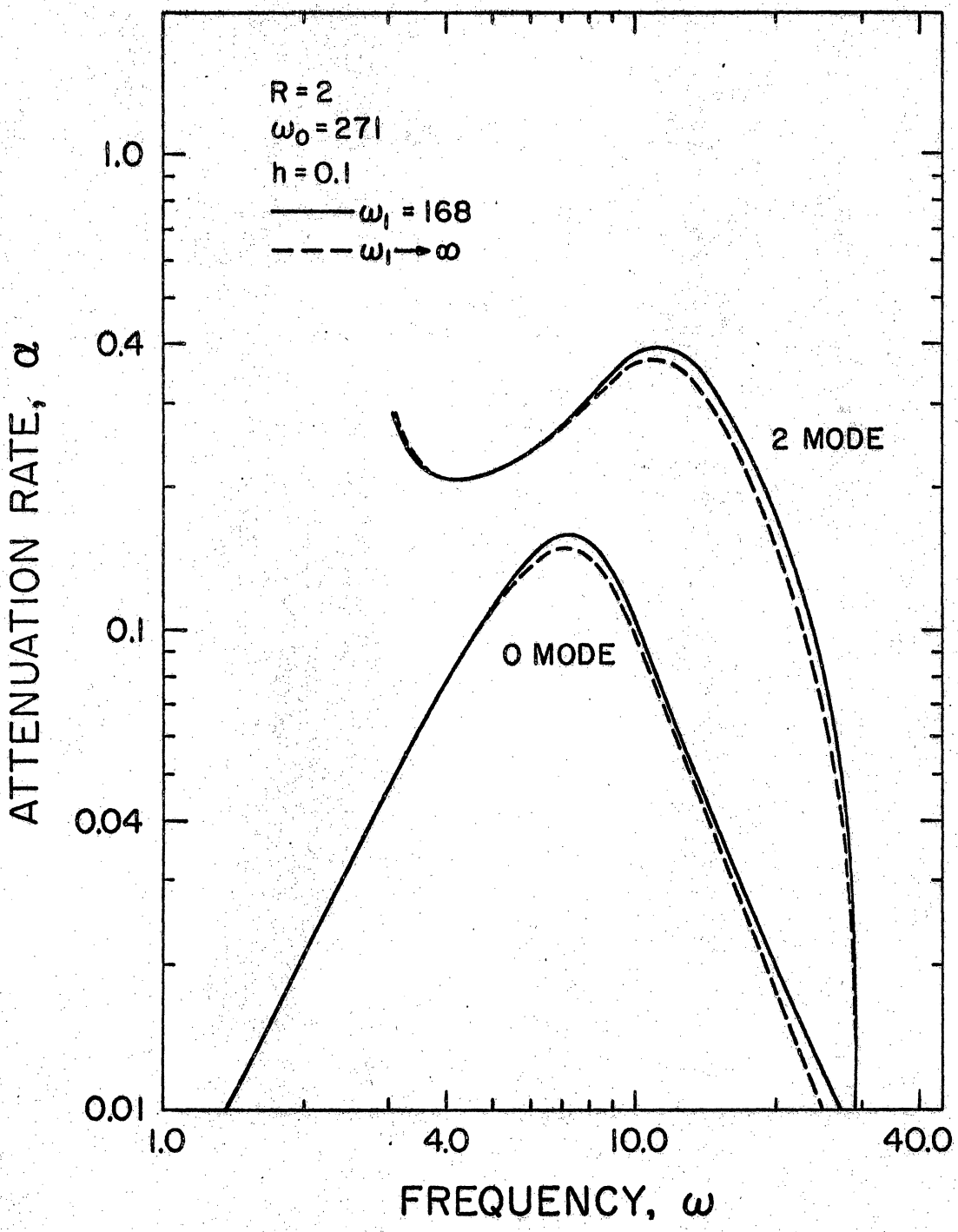

Figure 14. Comparison of the attenuation spectra predicted by the general formula (35) for the liner specific admittance to those predicted by the semi-empirical formula (36); very thin facing sheet, b = .005, h = 0.1, σ = 400, Ω = 0.95, s = 1.4, c_e = 0.91, M = 0.36.

the backing-cavity depth are frequently of the same magnitude. The agreement between the curves in Figures 12-14 would be improved somewhat if smaller values of the porosity and larger values of the structure factor were used. Nevertheless, it appears that the general formulation of the specific admittance is required to accurately predict the attenuation spectrum for a liner of moderate thickness.

5. Summary

The acoustic characteristics of a point-reacting duct liner that consists of a porous facing sheet backed by cellular cavities have been derived by examining the wave propagation within the liner, and the effect of the liner on sound propagation in a duct has been calculated for the case of a plane duct that carries a uniform mean flow.

For the case of no mean flow and no backing cavity, the derived expression for the liner specific admittance leads to attenuation rates that agree quantitatively with those of Kurze and Vér. These results for no backing cavity have been extended to cases of both upstream and downstream propagation in a uniform mean flow. The attenuation rates that are produced by the layer of porous material are shown to be very sensitive to the mean-flow Mach number.

The influence of the cavity depth and the thickness of the facing sheet on the attenuation rates of downstream-propagating modes have been examined for constant porous-material properties. For the cases considered, the attenuation of the two lowest modes can be raised to large levels by a proper choice of the cavity depth but the response of the higher modes is less favorable. For shallow cavities, an increase in the thickness of the facing sheet is less effective in raising the attenuation of the lower modes than is an increase in the cavity depth; however, for the higher modes, the porous-sheet thickness may be more effective than the cavity depth. For moderate cavity depths, the overall attenuation level changes with increases in the facing-sheet thickness up to a value somewhat larger than the cavity depth. Further

increases in the thickness of the porous material do not change the overall attenuation level but do result in a shift in the peaks of the attenuation curve.

The derived expression for the liner specific admittance has been shown to reduce, in the limit as the facing-sheet thickness vanishes, to a semi-empirical formula that has seen widespread use in the literature. Numerical comparisons of the attenuation rates predicted by the two formulas for cases of finite facing-sheet thickness indicate that the approximate formula is inadequate in many cases of practical interest, specifically when the facing-sheet and cavity dimensions are of the same order.

REFERENCES

1. R.A. Mangiarotty 1970 *Journal of the Acoustical Society of America* **48**, 783-794. Acoustic-lining concepts and materials for engine ducts.
2. R.A. Scott 1946 *Proceedings of the Physical Society* **58**, 165-183. The absorption of sound in a homogeneous porous medium.
3. E.A. Leskov, G.L. Osipov and E.J. Yudin 1970 *Applied Acoustics* **3**, 47-56. Experimental investigations of splitter duct silencers.
4. A. Bokor 1969 *Journal of Sound and Vibration* **10**, 390-403. Attenuation of sound in lined ducts.
5. A. Bokor 1971 *Journal of Sound and Vibration* **14**, 367-373. A comparison of some acoustic duct lining material, according to Scott's theory.
6. J. Walsdorff 1971 *Seventh International Congress on Acoustics, Budapest*, paper 25A 6. Absorptionsschalldämpfer ohne Kassetteirung.
7. M. Mongy 1973 *Acustica* **28**, 243-247. Acoustical properties of porous materials.
8. V.J. Kurze and I.L. Vér 1972 *Journal of Sound and Vibration* **24**, 177-187. Sound attenuation in ducts lined with non-isotropic material.
9. D.H. Tack and R.F. Lambert 1965 *Journal of the Acoustical Society of America* **38**, 655-666. Influence of shear flow on sound attenuation in a lined duct.
10. A.H. Nayfeh, J. Sun and D.P. Telionis 1973 *AIAA* paper no. 73-227. Effect of bulk-reacting liners on wave propagation in ducts.
11. A.H. Nayfeh, J. E. Kaiser and D.P. Telionis 1973 *AIAA* paper no. 73-1153. The acoustics of aircraft engine duct systems.

12. P,M. Morse 1939 *Journal of the Acoustical Society of America* 11, 205-210. The transmission of sound inside pipes.

13. L. Cremer 1940 *Akustische Zeitschrift* 5, 57-76. Nachhallzeit und Dampfungsmass bei streifendem Einfall.

14. P.M. Morse and U. Ingard 1968 *Theoretical Acoustics*, 252-255. McGraw-Hill.

15. C. Zwikker and C.W. Kosten 1949 *Sound Absorbing Materials*, Elsevier Publ. Co., New York.

16. S.H. Ko 1971 *Journal of the Acoustical Society of America* 50, 1418-1432. Sound attenuation in lined rectangular ducts with flow and its application to the reduction of aircraft engine noise.

17. W. Eversman 1970 *Journal of the Acoustical Society of America* 48, 425-427. The effect of Mach number on the tuning of an acoustic lining in a flow duct.

18. B.J. Tester 1973 *Journal of Sound and Vibration* 28, 151-203. The propagation and attenuation of sound in lined ducts containing uniform or "plug" flow.

19. W.E. Zorumski and J.P. Mason, in Press, , *Journal of the Acoustical Society of America*. Multiple eigenvalues of sound absorbing circular and annular ducts.

The vita has been removed from the scanned document

ABSTRACT

The acoustic characteristics of a point-reacting duct liner that consists of a porous facing sheet backed by cellular cavities are derived by examining the wave propagation within the liner. The relation between the derived expression for the liner acoustic admittance and a semi-empirical formula that is widely used in the literature is discussed. The influence of the liner on acoustic propagation in a duct is examined for the case of a plane duct that carries a uniform mean flow. Numerical results for the attenuation rates vs. frequency are presented. These results are of three types: (1) comparisons with previously published results for no backing cavity and no mean flow are made, and these results are extended to include the effects of the mean flow; (2) results of parametric variations of the liner dimensions are presented to assess the relative influence of the facing-sheet thickness and the cavity depth; (3) results from the derived expression for liner specific admittance and from the semi-empirical formula are compared in order to determine the significance of the wave propagation within the porous material and to determine the range of validity of the semi-empirical formula.